Proceedings of the 9th International Conference on Fluid Flow, Heat and Mass Transfer (FFHMT'22)
Niagara Falls, Canada – June 08-10, 2022
Paper No. 214
DOI: 10.11159/ffhmt22.214

The Influence of Tio_2 Nanoparticles and Libr on the Exergy Efficiency of Ammonia Absorption Refrigeration System under Different Working Temperatures

Jin Zhenghao[1], Shuhong Li[1,*], Kai Du[1]
[1]School of Energy and Environment, Southeast University,
No 2 Sipailou, Nanjing 210096, China
230189430@seu.edu.cn

Abstract - The addition of TiO_2 nanoparticles and LiBr can increase the coefficient of performance(COP) of the ammonia water absorption, but the exergy efficiency has not been investigated. Therefore, this paper studied the influence of TiO_2 nanoparticles and LiBr on the exergy efficiency under different working temperatures. The results show that the addition of TiO_2 nanoparticles or LiBr can improve the ECOP of the ammonia-water absorption refrigeration system. There is optimal T_{gen}, T_{eva} for the NH_3-H_2O-LiBr-TiO_2 working fluid, which is 110℃, -13℃. In comparison, the ECOP decreases with the T_{cw} increases. The maximum value of ECOP in this paper is 0.266 when the T_{eva}, T_{gen}, and T_{cw} are -13℃, 110℃, and 28℃. Generally, applying NH_3 – H_2O - LiBr – TiO_2 nanofluid working fluid can efficiently improve the ECOP of the absorption refrigeration system.

Keywords: absorption refrigeration, exergy, experimental investigation

Nomenclature			
E	Exergy, W	*T*	Temperature, °C
ECOP	Exergy coefficient of performance	T_0	Environment temperature, °C
p	Pressure, MPa	T_1, T_2, …T_{18}	Value of each temperature test point, °C
p_1, p_2, …p_6	Value of each pressure test point, MPa	*m*	Mass, kg
P	Power, W	*x*	Concentration in the liquid phase, kg/kg
q	Mass flow, kg/h^{-1}		
Subscripts			
gen	Generator	*con*	Condenser
eva	Evaporator	*p*	Pump
cw	Cooling water	*LiBr*	Lithium bromide
abs	Absorber	*TiO2*	Titanium dioxide

1. Introduction

Absorption refrigeration system (ARS) is a promising technology applied in the waste heat recovery field[1, 2] and solar thermal utilization field[3, 4]. Ammonia-water (NH_3-H_2O) working pair has a bigger application range than the water-lithium bromide (H_2O-LiBr) working pair[5] and is well used in the ARS. But it requires a rectification process to separate the water vapor mixed with ammonia gas, which consumes a lot of heat and decreases the COP of the system. Adding salts (like NaOH[6] [7], $LiNO_3$[8] [9] [10], LiBr[11][12]) to the ammonia water can reduce the water mix into the ammonia vapor gas in the generator because it enhanced the separation of ammonia in the generator and reduced the chiller driving temperature by taking advantage of the common ion effect.

Nanofluid application in the ARS improves heat transfer and mass transfer efficiencies of the devices in the experimental system, so the ammonia absorbed by the weak solution in the absorber is increased, and the system COP is enhanced. In existing studies, the heat transfer of the heat exchanger was improved by 22.0%[13], 29.8%[14], or 18.5-27.2%[15] by adding TiO_2, Al_2O_3, or CuO nanoparticles to basic liquid. The falling film absorption rate was improved by 70% and 50% by adding Fe_2O_3 and $ZnFe_2O_4$ nanoparticles. Furthermore, adding TiO_2 can improve the NH_3-H_2O ARS and NH_3-H_2O-LiBr ARS by 27%[16, 17] and 19%[18], respectively.

Exergy analysis is also an effective thermodynamic tool used to analyze complex thermal systems such as absorption refrigeration systems [19], Organic Rankine Cycle[20], heat pump systems [21], and so on. Exergy analysis estimates the efficiency, energy quality, and available works in a system [22], giving the ability to specify the maximum performance[23]. The irreversible energy loss of the system is decreased when the exergy efficiency is increased. Therefore, we often seek the best exergy efficiency to reduce the irreversible energy loss of the system, optimizing the system operation modes.

In our previous studies, the coefficient of performance(COP) increases when the generation temperature or evaporation temperature increases. But the irreversible energy losses are not clear and need further discussion. This time the influence of TiO_2 nanoparticles and LiBr on the exergy efficiency of the ammonia ARS is investigated under different generation, evaporation, and cooling water temperatures. The working condition makes the exergy coefficiency of performance(ECOP) the highest is found to reduce the irreversible loss of the system.

2. Methods

2.1 Description of the experimental ARS system

The experimental ARS is a typical single-effect absorption refrigeration system built in Shandong, China. The main body of the experimental absorption refrigeration cycle is shown in Fig. 1. The generator, the absorber, the evaporator, the condenser, the pipes, and other devices in the experimental system are all made of stainless steel to avoid the corrosion of ammonia water. Several electric heaters are installed at the bottom of the generator and evaporator. The expected generation power and evaporation power can be obtained by adjusting the power of these electric heaters. The distillation column is packed with metal stainless steel structured packing, and it is connected to the reflux condenser to collect refluxed ammonia water. A falling film type absorber is adopted because it has a good performance when using nanofluid. Throttle valves control the pressure drop and the flux of the ammonia or ammonia-water solution. Other valves control the working medium in the system, such as filling ammonia into the system, filling nanofluid into the system, checking funneled point, etc. The generator, rectifier, condenser, and connecting pipes are wrapped with thermal insulation materials to reduce heat transfer with the surrounding environment. The cooling water flow rates(Q_1~Q_3), temperatures(T_1~T_{18}), pressures(p_1~p_5), and power consumption of the evaporator and generator are monitored and recorded by a compiled program from Visual Basic. A parallel cooling water circulation precisely controls the cooling water temperature(T_{cw}=T_{15}). The evaporation temperature is tested by test point 6 (T_{eva}=T_6), and the generation temperature is tested by test point 1 (T_{gen}=T_1).

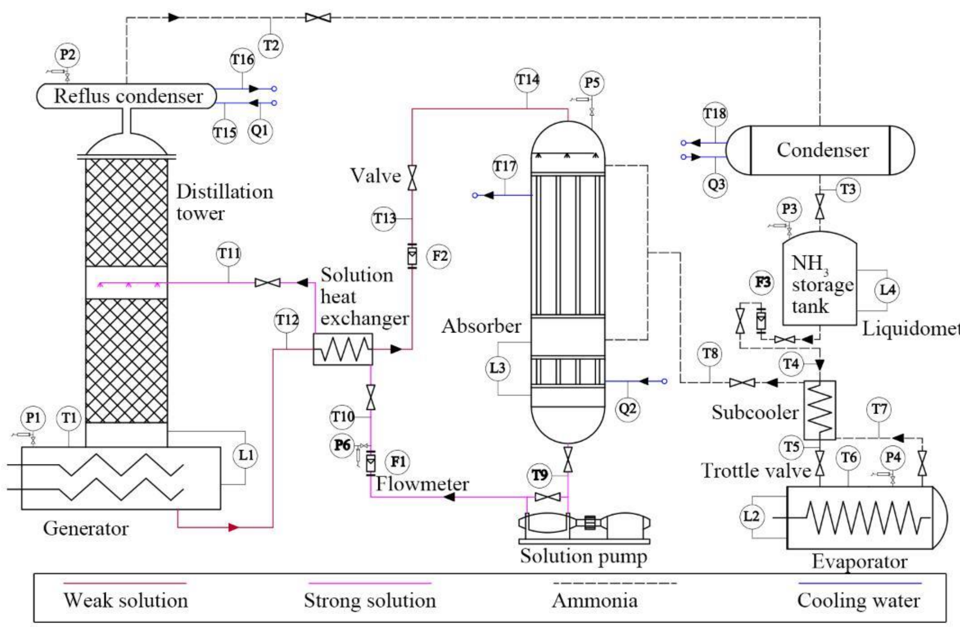

Fig. 1. The schematic diagram of the absorption refrigeration cycle

2.2 Experimental Methods

The performance of the ammonia-water ARS is tested under the designed working condition. The generation temperature is varied from 100℃ to 130℃. The evaporation temperature is varied from -19℃ to -2℃. The cooling water temperature is varied from 21℃ to 33℃.

At the beginning of each experiment, the cooling water temperature (T_{15}) is kept stable by adjusting the cooling water system. After that, generation power, evaporation power, and throttle valves are adjusted to make T_1, T_9, T_6, T_3 at the designed working condition. The liquid level of the generator, evaporator, the NH_3 storage tank, and the T_1, T_9, T_6, T_3 are kept stabilized for at least 30min before recording to keep the working condition stable. After that, the flows, temperatures, pressures, and power consumption of the evaporator and generator are recorded for 20min.

The working fluid in this paper has four types, which are NH_3-H_2O working fluid (x_{LiBr}=0%, x_{TiO2}=0%), NH_3-H_2O-TiO_2 working fluid(x_{LiBr}=0%, x_{TiO2}=0.5%), NH_3-H_2O-LiBr working fluid (x_{LiBr}=15%, x_{TiO2}=0%), and NH_3-H_2O-LiBr-TiO_2 working fluid (x_{LiBr}=15%, x_{TiO2}=0.5%). The experimental data of NH_3-H_2O working fluid and NH_3-H_2O-TiO_2 working fluid is published by Jiang[17]. The experimental data of NH_3-H_2O-LiBr working fluid is published by Xu[11]. The experimental data of NH_3-H_2O-LiBr-TiO_2 working fluid is the most recent tested. The information on the LiBr and TiO_2 nanoparticles is listed in Table.1.

Table.1. Parameters of the LiBr and TiO_2 nanoparticles added to ammonia-water in the experiment

LiBr			
Color:	White powder	Manufacture factory:	Aladdin (China)
Purity:	99.9% metals basis	Product number:	L108934-500 g
TiO_2 nanoparticles			
Crystal shape:	Rutile type	Manufacture factory:	XFNANO (China)
Particle size:	5-10nm	Product number:	XFI21
Purity:	99.3 wt % metals basis		

2.3 Uncertainty of the experimental data

A typical experiment result is shown in table 2, in which the temperatures, pressures, and energy consumptions of the generator and evaporator are listed. The x_{LiBr}, x_{TiO2} are 15%, 0.5%, and the temperature of the generator, the evaporator, and the cooling water are 110.05℃, -10.03℃, and 27.5℃. The uncertainty analysis listed in table 2 is conducted according to Wu et al. [24]. The total uncertainty consists of system uncertainty and random uncertainty. The uncertainty analysis results show that the experimental system's measurement error is very small.

Table. 2. The experiment result and the uncertainty analysis under the typical working condition.

Parameter	Average value	System uncertainty	Random uncertainty	Total uncertainty	Parameter	Average value	System uncertainty	Random uncertainty	Total uncertainty
T_1	110.05℃	±0.1℃	±0.16℃	±0.26℃	T_{16}	29.69℃	±0.1℃	±0.02℃	±0.12℃
T_2	36.56℃	±0.1℃	±0.05℃	±0.15℃	T_{17}	31.25℃	±0.1℃	±0.03℃	±0.13℃
T_3	30.49℃	±0.1℃	±0.03℃	±0.13℃	T_{18}	28.93℃	±0.1℃	±0.03℃	±0.13℃
T_4	30.61℃	±0.1℃	±0.04℃	±0.14℃	p_1	1.200MPa	±3kPa	±0.47kPa	±3.47kPa
T_5	17.74℃	±0.1℃	±0.27℃	±0.37℃	p_2	1.202 MPa	±3kPa	±0.47kPa	±3.47kPa
T_6	-10.03℃	±0.1℃	±0.14℃	±0.24℃	p_3	1.197 MPa	±3kPa	±0.46kPa	±3.46kPa
T_7	0.53℃	±0.1℃	±0.05℃	±0.15℃	p_4	0.273 MPa	±0.9kPa	±0.39kPa	±1.29kPa
T_8	31.35℃	±0.1℃	±0.08℃	±0.18℃	p_5	0.270 MPa	±0.9kPa	±0.36kPa	±1.26kPa
T_9	35.94℃	±0.1℃	±0.04℃	±0.14℃	p_6	1.307 MPa	±3kPa	±0.27kPa	±5.70kPa
T_{10}	36.33℃	±0.1℃	±0.04℃	±0.14℃	P_{gen}	3815.46W	±11.45W	±24.46W	±35.91W
T_{11}	88.51℃	±0.1℃	±0.13℃	±0.23℃	P_{eva}	1717.52W	±5.15W	±18.27W	±23.42W
T_{12}	109.61℃	±0.1℃	±0.06℃	±0.16℃	P_p	537.23W	±1.61W	±4.58W	±6.19W
T_{13}	42.45℃	±0.1℃	±0.14℃	±0.24℃	$q_{cw,abs}$	960 kg/h	±1kg/h	±1kg/h	±2kg/h
T_{14}	41.70℃	±0.1℃	±0.13℃	±0.23℃	$q_{cw,con}$	1000 kg/h	±1kg/h	±1kg/h	±2kg/h
T_{15}	27.49℃	±0.1℃	±0.02℃	±0.12℃					

2.4 Calculation methods of Exergy Coefficient Of Performance (ECOP)

The Exergy Coefficient Of Performance (ECOP) is the exergy produced by the evaporator(E_{eva}) divided by the exergy consumed by the generator(E_{gen}). The E_{eva} is calculated by the evaporation heat(P_{eva}), the evaporation temperature(T_{eva}=T_6), and the environment temperature(T_0=24.5°C). While the E_{gen} is calculated by the generation heat(P_{gen}), the generation temperature(T_{gen}=T_1), and the environment temperature(T_0=24.5°C)[25].

$$\text{ECOP} = \frac{E_{eva}}{E_{gen}} \quad (1)$$

$$E_{eva} = P_{eva}\left(\frac{273.15 + T_0}{273.15 + T_{eva}} - 1\right) \quad (2)$$

$$E_{gen} = P_{gen}\left(1 - \frac{273.15 + T_0}{273.15 + T_{gen}}\right) \quad (3)$$

The concentrations of LiBr and TiO_2 are defined as equations (4) and (5). It is convenient to calculate the charging mass of LiBr and TiO_2 to the system.

$$x_{LiBr} = \frac{m_{LiBr}}{m_{H_2O} + m_{LiBr}} \quad (4)$$

$$x_{TiO_2} = \frac{m_{TiO_2}}{m_{H_2O} + m_{TiO_2}} \quad (5)$$

3. Results and discussions

3.1 Influence of the T_{eva} on the E_{eva}, E_{gen}, and ECOP

The influences of the T_{eva} on the E_{eva}, E_{gen} are shown in Fig. 2. The E_{eva} and E_{gen} increase when the T_{eva} increase. It is because the P_{eva} and P_{gen} increase when the evaporation temperature is increased. Besides, the increasing rate of the E_{gen} is higher than the E_{eva}. The increase of T_{eva} is bad for E_{eva}, which is in the denominator of the E_{eva}.

The influences of the T_{eva} on the ECOP are shown in Fig. 3. The black curve is the largest, indicating that the exergy efficiency of the NH_3-H_2O-LiBr-TiO_2 working fluid is higher than the other three groups. The curves when x_{LiBr}/x_{TiO2} are 15%/0.5% and 15%/0% increase first and decrease after catching the maximum value when the T_{eva} increases. The maximum ECOPs of the two groups are 0.266 and 0.235, respectively, when the values of T_{eva} are -13°C and -10°C. They are the best evaporation temperature with the minimum irreversible loss of the two working fluids. But the other two curves decrease straightly with the T_{eva} increases. Because the generation temperature of the two groups is higher and has a stronger refrigeration capacity, the optimal evaporation temperatures of these two working fluids are properly less than 19°C.

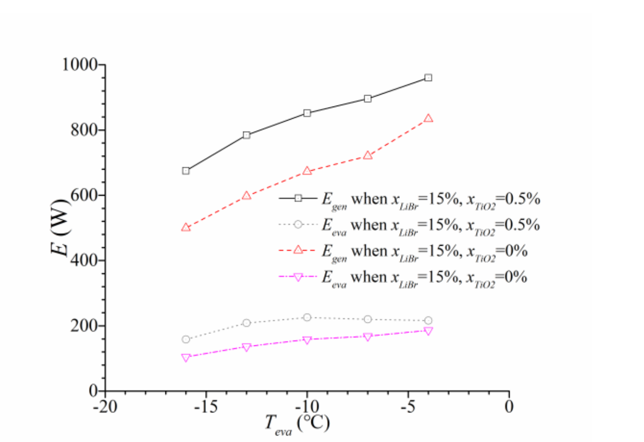

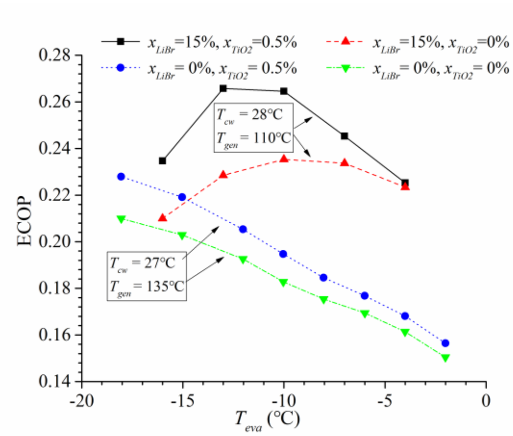

Fig. 2. The E_{gen} and E_{eva} vary with the T_{eva}

Fig. 3. The ECOP varies with the T_{eva}

3.2 Influence of the T_{gen} on the E_{eva}, E_{gen}, and ECOP

The influences of the T_{gen} on the E_{eva}, E_{gen} are shown in Fig. 4. The E_{eva} and E_{gen} increase when the T_{gen} increase. That is because the P_{eva} and P_{gen} increase when the T_{gen} is increased. Besides, the increasing rate of the E_{gen} is higher than the E_{eva}. Because the increase of T_{gen} is good for E_{eva}, shown in equation 3.

The influences of the T_{gen} on the ECOP are shown in Fig. 5. The ECOP of the NH_3-H_2O-LiBr-TiO_2 working fluid is also higher than the other three groups. The curves all increase first and decrease after catching the maximum value with the T_{gen} increases. The maximum ECOP is 0.264 when $x_{\text{LiBr}}/x_{\text{TiO2}}$=15%/0.5% and T_{gen}=110℃. While the two groups when x_{LiBr} =0% catch maximum value when T_{gen}=115℃, rather than 110℃. It is because the optimal T_{gen} increases when the cooling water temperature increases.

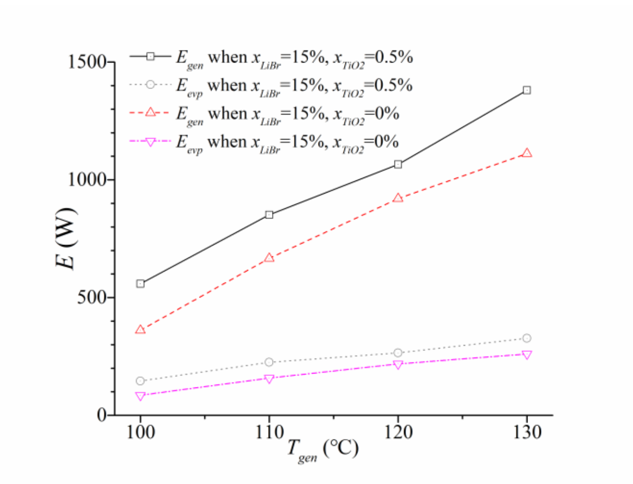

Fig. 4. The E_{gen} and E_{eva} vary with the T_{gen}

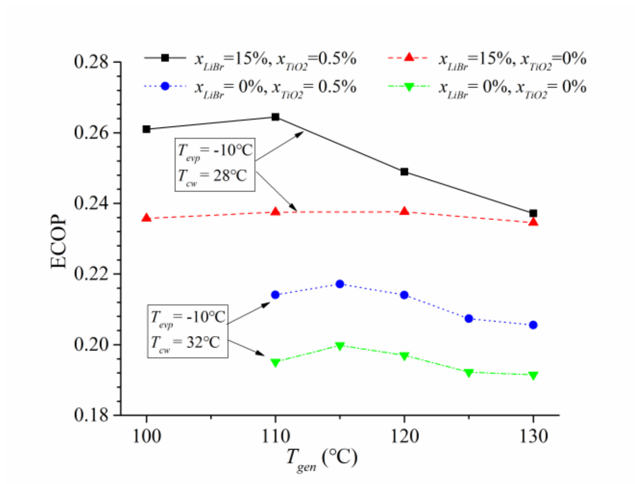

Fig. 5. The ECOP varies with the T_{gen}

3.3 Influence of the T_{cw} on the E_{eva}, E_{gen}, and ECOP

The influences of the T_{cw} on the E_{eva}, E_{gen} are shown in Fig. 6. The E_{eva} and E_{gen} decrease when the T_{cw} increase. Because system cooling capacity decreases when the cooling water temperature increases. The influences of the T_{cw} on the ECOP are shown in Fig. 7. The ECOP of the NH_3-H_2O-LiBr-TiO_2 working fluid is also higher than the other three groups. The curves all decrease with the T_{cw} increases, showing that the irreversible loss of the system increases with the T_{cw} increases.

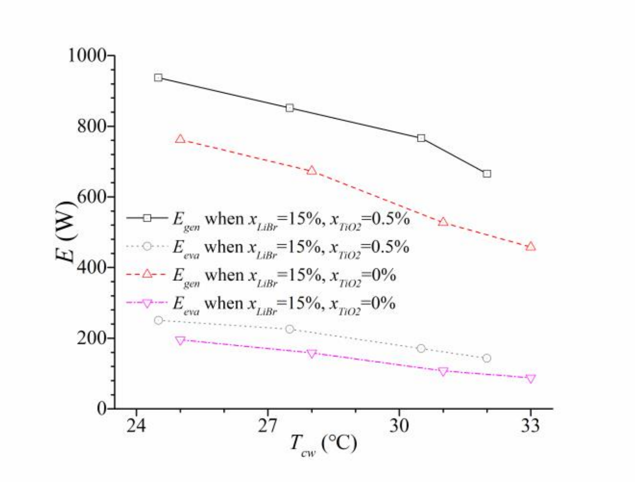

Fig. 6. The E_{gen} and E_{eva} vary with the T_{cw}

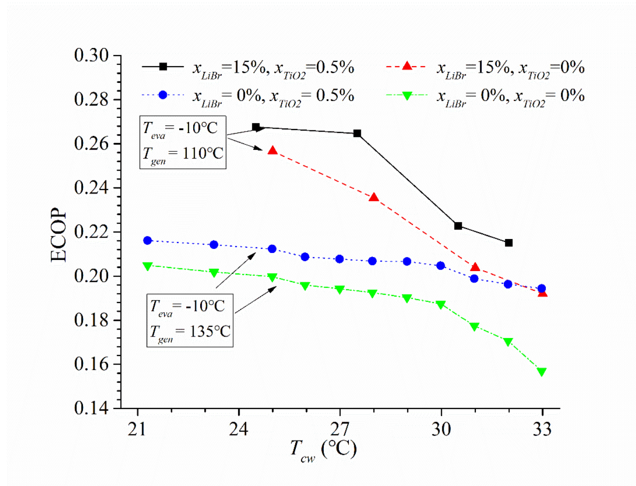

Fig. 7. The ECOP varies with the T_{cw}

4. Conclusion

This paper experimentally investigated the influence of TiO_2 nanoparticles and LiBr on the exergy efficiency of the ammonia ARS under different generation, evaporation, and cooling water temperatures. The following conclusions can be obtained according to the experimental results.

1. The ECOP of the NH_3-H_2O-LiBr-TiO_2 working fluid is higher than the other three working fluids under the same T_{cw}, T_{gen}, T_{eva}.

2. The E_{eva}, E_{gen} increase when the T_{eva}, T_{gen} increase or the T_{cw} decrease.

3. The ECOP for the NH_3-H_2O-LiBr-TiO_2 working fluid increases first and decreases after catching the maximum value when the T_{eva} increases. The maximum ECOPs are 0.266 when the values of T_{eva} are -13°C. The ECOPs for the NH_3-H_2O-TiO_2 and NH_3-H_2O working fluid decrease when the T_{eva} increases from -19°C to -2°C. The optimal evaporation temperatures of the two working fluids are possibly less than -19°C.

4. The ECOPs of the four working fluids increase first and decrease after catching the maximum value when the T_{gen} increases. The optimal values of T_{gen} for the four groups are between 110~115°C.

5. The ECOPs decrease with the T_{cw} increases, showing that the irreversible loss of the system increases with the T_{cw} increases.

The addition of TiO_2 nanoparticles and LiBr can improve the ECOP of the ammonia-water absorption refrigeration system. Our experimental results find that 110°C and -13°C are optimal T_{gen} and T_{eva} for the NH_3-H_2O-LiBr-TiO_2 working fluid. The ECOP will catch maximum value under such conditions.

Acknowledgements

The work of this paper is financially supported by the National Natural Science Foundation of China (No. 51876033).

References:

[1] C. Zhai and W. Wu, "Performance optimization and comparison towards compact and efficient absorption refrigeration system with conventional and emerging absorbers/desorbers," *Energy,* vol. 229, p. 120669, 2021.

[2] Y. Gao, G. He, P. Chen, X. Zhao, and D. Cai, "Energy and exergy analysis of an air-cooled waste heat-driven absorption refrigeration cycle using R290/oil as working fluid," *Energy,* vol. 173, pp. 820-832, 2019.

[3] E. Dai, T. Jia and Y. Dai, "Theoretical and experimental investigation on a GAX-Based NH3-H2O absorption heat pump driven by parabolic trough solar collector," *Solar Energy,* vol. 197, pp. 498-510, 2020.

[4] A. Khaliq, R. Kumar and E. M. A. Mokheimer, "Investigation on a solar thermal power and ejector-absorption refrigeration system based on first and second law analyses," *Energy,* vol. 164, pp. 1030-1043, 2018.

[5] E. Bellos, I. Chatzovoulos and C. Tzivanidis, "Yearly investigation of a solar-driven absorption refrigeration system

with ammonia-water absorption pair," *Thermal Science and Engineering Progress,* vol. 23, p. 100885, 2021.

[6] S. Steiu, D. Martínez-Maradiaga, D. Salavera, J. C. Bruno, and A. Coronas, "Effect of Alkaline Hydroxides on the Vapor−Liquid Equilibrium of Ammonia/Water and the Performance of Absorption Chillers," *Industrial & Engineering Chemistry Research,* vol. 50, pp. 13037-13044, 2011-12-07 2011.

[7] S. Steiu, D. Salavera, J. C. Bruno, and A. Coronas, "A basis for the development of new ammonia–water–sodium hydroxide absorption chillers," *International Journal of Refrigeration,* vol. 32, pp. 577-587, 2009.

[8] J. Cerezo, R. Best and R. J. Romero, "A study of a bubble absorber using a plate heat exchanger with NH3–H2O, NH3–LiNO3 and NH3–NaSCN," *Applied Thermal Engineering,* vol. 31, pp. 1869-1876, 2011.

[9] D. Cai, J. Jiang, G. He, K. Li, L. Niu, and R. Xiao, "Experimental evaluation on thermal performance of an air-cooled absorption refrigeration cycle with NH 3 –LiNO 3 and NH 3 –NaSCN refrigerant solutions," *Energy Conversion and Management,* vol. 120, pp. 32-43, 2016.

[10] X. Liang, S. Zhou, J. Deng, G. He, and D. Cai, "Thermodynamic analysis of a novel combined double ejector-absorption refrigeration system using ammonia/salt working pairs without mechanical pumps," *Energy,* vol. 185, pp. 895-909, 2019.

[11] M. Xu, S. Li, Z. Jin, W. Jiang, and K. Du, "Experimental investigation of the effect of LiBr on the high-pressure part of a ternary working fluid ammonia absorption refrigeration system," *Applied Thermal Engineering,* vol. 186, p. 116521, 2021.

[12] R. Peters, C. Korinth and J. U. Keller, "Vapor-Liquid Equilibria in the System NH3 + H2O + LiBr. 2. Data Correlation," *Journal of Chemical & Engineering Data,* vol. 40, pp. 775-783, 1995-01-01 1995.

[13] A. R. Sajadi and M. H. Kazemi, "Investigation of turbulent convective heat transfer and pressure drop of TiO2/water nanofluid in circular tube," *International Communications in Heat and Mass Transfer,* vol. 38, pp. 1474-1478, 2011.

[14] R. Barzegarian, A. Aloueyan and T. Yousefi, "Thermal performance augmentation using water based Al 2 O 3 -gamma nanofluid in a horizontal shell and tube heat exchanger under forced circulation," *International Communications in Heat and Mass Transfer,* vol. 86, pp. 52-59, 2017.

[15] M. A. Khairul, M. A. Alim, I. M. Mahbubul, R. Saidur, A. Hepbasli, and A. Hossain, "Heat transfer performance and exergy analyses of a corrugated plate heat exchanger using metal oxide nanofluids," *International Communications in Heat and Mass Transfer,* vol. 50, pp. 8-14, 2014.

[16] W. Jiang, S. Li, L. Yang, and K. Du, "Experimental investigation on enhancement of ammonia absorption process with TiO2 nanoparticles in newly designed absorber," *International Journal of Refrigeration,* vol. 100, pp. 93-103, 2019.

[17] W. Jiang, S. Li, L. Yang, and K. Du, "Experimental investigation on performance of ammonia absorption refrigeration system with TiO2 nanofluid," *International Journal of Refrigeration,* vol. 98, pp. 80-88, 2019.

[18] Z. Jin, S. Li, R. Zhou, M. Xu, W. Jiang, and K. Du, "Experimental investigation on the effect of TiO2 nanoparticles on the performance of NH3 – H2O - LiBr absorption refrigeration system," *International Journal of Refrigeration,* vol. 131, pp. 826-833, 2021.

[19] S. Mohtaram, M. Omidi, J. Lin, H. Sun, and W. Chen, "Exergy analysis of a multi mixture working fluid absorption refrigeration cycle," *Case Studies in Thermal Engineering,* vol. 15, p. 100540, 2019.

[20] M. Fallah, Z. Mohammadi and S. M. S. Mahmoudi, "Advanced exergy analysis of the combined S–CO2/ORC system," *Energy,* vol. 241, p. 122870, 2022.

[21] J. Cai, H. Zhou, L. Xu, Z. Shi, T. Zhang, and J. Ji, "Energy and exergy analysis of a novel solar-air composite source multi-functional heat pump," *Renewable energy,* vol. 185, pp. 32-46, 2022-01-01 2022.

[22] O. Mahian, M. R. Mirzaie, A. Kasaeian, and S. H. Mousavi, "Exergy analysis in combined heat and power systems: A review," *Energy Conversion and Management,* vol. 226, p. 113467, 2020.

[23] R. Saidur, G. BoroumandJazi, S. Mekhilef, and H. A. Mohammed, "A review on exergy analysis of biomass based fuels," *Renewable and Sustainable Energy Reviews,* vol. 16, pp. 1217-1222, 2012.

[24] W. Wu, S. Ran, W. Shi, B. Wang, and X. Li, "NH3-H2O water source absorption heat pump (WSAHP) for low temperature heating: Experimental investigation on the off-design performance," *Energy,* vol. 115, pp. 697-710, 2016.

[25] R. Haghbakhsh, H. Peyrovedin, S. Raeissi, A. R. C. Duarte, and A. Shariati, "Investigating the performance of novel

green solvents in absorption refrigeration cycles: Energy and exergy analyses," *International Journal of Refrigeration,* vol. 113, pp. 174-186, 2020.